Journal of Cultural Heritage 54 (2022) 21–30

Contents lists available at ScienceDirect

Journal of Cultural Heritage

journal homepage: www.elsevier.com/locate/culher

Original article

Systematic calculation of flying buttress parameters by means of geometric regression

Albert Samper[a,1], Blas Herrera[b,2,*], Agustí Costa-Jover[c,3]

[a] Universitat Rovira i Virgili and IRH-UDG, Escola Tècnica Superior d'Arquitectura, Reus, Spain
[b] Universitat Rovira i Virgili, Departament d'Enginyeria Informàtica i Matemàtiques, Tarragona, Spain
[c] Universitat Rovira i Virgili, Escola Tècnica Superior d'Arquitectura, Reus, Spain

ARTICLE INFO

Article history:
Received 20 September 2021
Accepted 9 January 2022
Available online 22 January 2022

Keywords:
Flying buttresses
Gothic cathedrals
Geometric regression
Viollet-le-Duc

ABSTRACT

This paper investigates the geometric parameters of a flying buttress: position of the center $\mathcal{O}$ of the intrados arch, radius $\mathcal{R}$ of the intrados arch, inclination α, rise $\mathcal{F}$, span distance $\mathcal{L}$ and horizontal thickness $\mathcal{E}$ of the culée. Using photogrammetrical techniques, point cloud control, vector redrawing and geometric regression, this paper provides an objective, non-arbitrary procedure to determine the center $\mathcal{O}$ and the radius $\mathcal{R}$ of a flying buttress arch. This results in two outcomes: 1) Non-arbitrary determination of the remaining parameters α, $\mathcal{F}$, $\mathcal{L}$ and $\mathcal{E}$; 2) Non-arbitrary classification of flying buttress arches into two types, according to the criterion laid down by Viollet-le-Duc in 1854.

1. Introduction

The construction of churches and Gothic cathedrals is a complex issue which has drawn the attention of many researchers in recent history. There are scarcely any historical records from the Gothic period which address design issues, and the few existing documents in this regard date from the late Gothic period [1]. Several investigations on the history of construction were conducted in the mid-nineteenth century, such as the papers by Robert Willis [2] (Willis, 1842) and Auguste Choisy [3], among many others, but Viollet-le-Duc [4] was the first researcher who presented a complete theory on Gothic construction. This paper intends to further knowledge in this area, focusing on one of the most representative elements of Gothic architecture: the flying buttress.

Recent monographic investigations on flying buttresses are extremely scarce. The papers written by Eugène Lefèvre-Pontalis [5], Jackes Heyman [6] and Robert Mark [7] –the two latter focusing on the overall stability of buildings– were the precursors to research on these architectural elements. John Fitchen also looked at the construction of Gothic cathedrals and specifically analyzed the behavior of flying buttresses [8,9]. Other more recent investigations, such as [10] and [1, 11], also furthered the structural analysis of these buildings and examined their design and proportions.

Recent investigations specifically dealing with flying buttresses include several papers focused on structural matters, such as [12] and [13], who provided a method to analyze flying buttresses based on Heyman's approach. The authors of reference [14] developed a method of analysis based on compression lines, complementing their structural analysis with a study of the geometric layout of the intrados arch. Later, [15] examined flying buttresses from a purely geometric point of view, and provided a method to study arches having two centers.

A flying buttress is determined by the following geometric parameters: position of the center $\mathcal{O}$ of the intrados arch, radius $\mathcal{R}$ of the intrados arch, inclinationα, rise $\mathcal{F}$, span distance $\mathcal{L}$ and horizontal thickness $\mathcal{E}$ of the culée. These parameters can be seen in Fig. 1. From a geometric point of view, we will show that all these parameters are determined by the center $\mathcal{O}$ and the radius $\mathcal{R}$ of the circle which defines the intrados arch of the flying buttress. In theory, it would be enough to choose three random points from the edge contour of the intrados arch and then draw the perpendicular bisectors of the resulting segments in order to determine $\mathcal{O}$ and $\mathcal{R}$. However, this method is not so evident or valid, as will be made clear later in this paper.

The lack of accuracy during the construction process, the deterioration due to the passing of time, seismic disturbances, structural deformations and other incidents of diverse nature may result in a change of the geometric type of the arch which was originally designed, and may also cause that the arch's center $\mathcal{O}$ and the arch radius $\mathcal{R}$ vary depending on the three points which are chosen.

* Corresponding authors.
E-mail addresses: albert.samper@urv.cat (A. Samper), blas.herrera@urv.cat (B. Herrera), agusti.costa@urv.cat (A. Costa-Jover).
[1] Orcid: 0000–0002–4795–2127
[2] Orcid: 0000–0003–2924–9195.
[3] Orcid: 0000–0002–6194–3243

https://doi.org/10.1016/j.culher.2022.01.005
1296-2074/

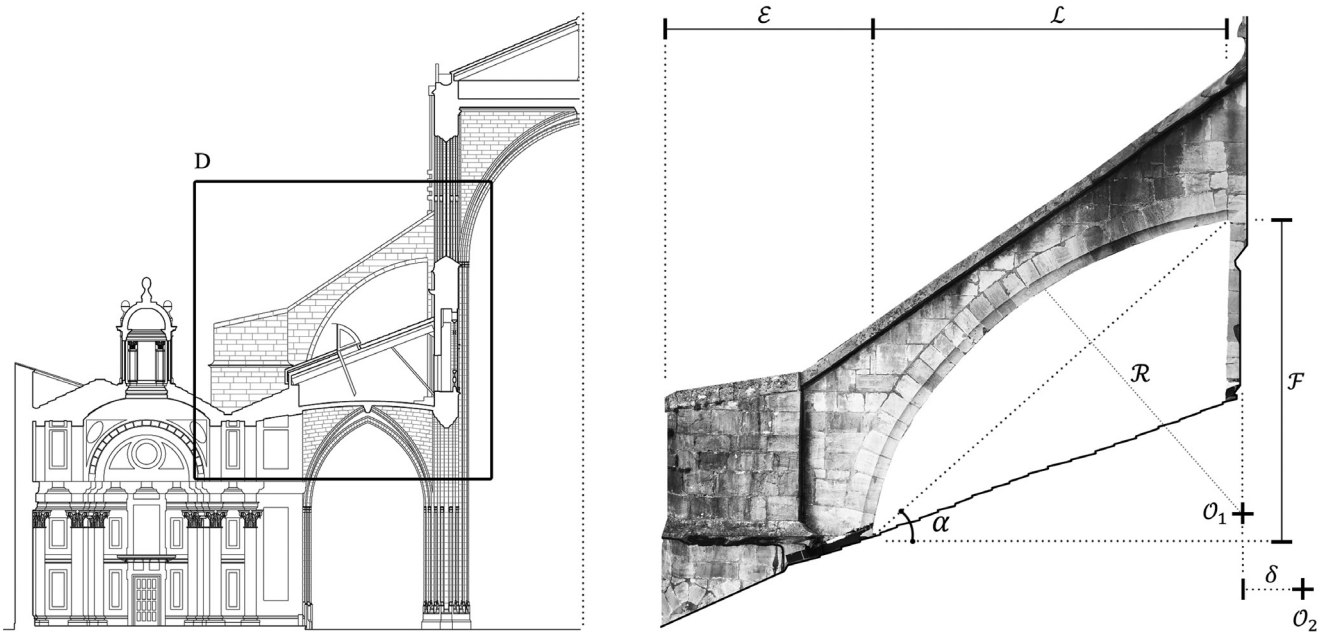

Fig. 1. On the left, cross section of Oviedo Cathedral, where box D delimits the photogrammetric reconstruction on the right. This reconstruction shows the parameters which define the flying buttresses. Case O1 corresponds to an intrados arch having its center on the wall, and case O2 corresponds to an intrados arch having its center inside the cathedral. [Image created by the authors].

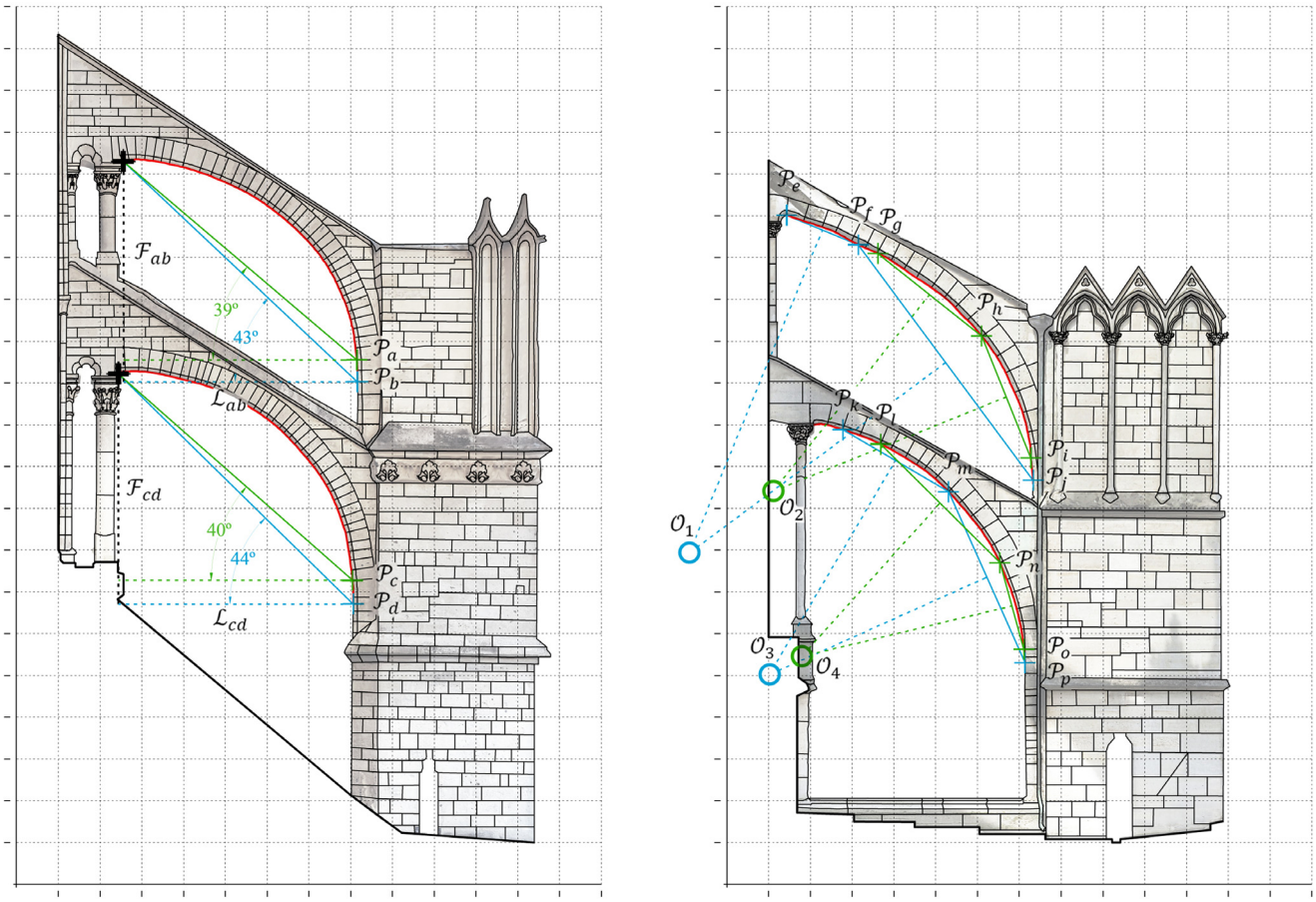

Fig. 2. On the left, graphic representation of a flying buttress from Amiens cathedral. On the right, graphic representation of a flying buttress from Saint Denis cathedral. [Image created by the authors].

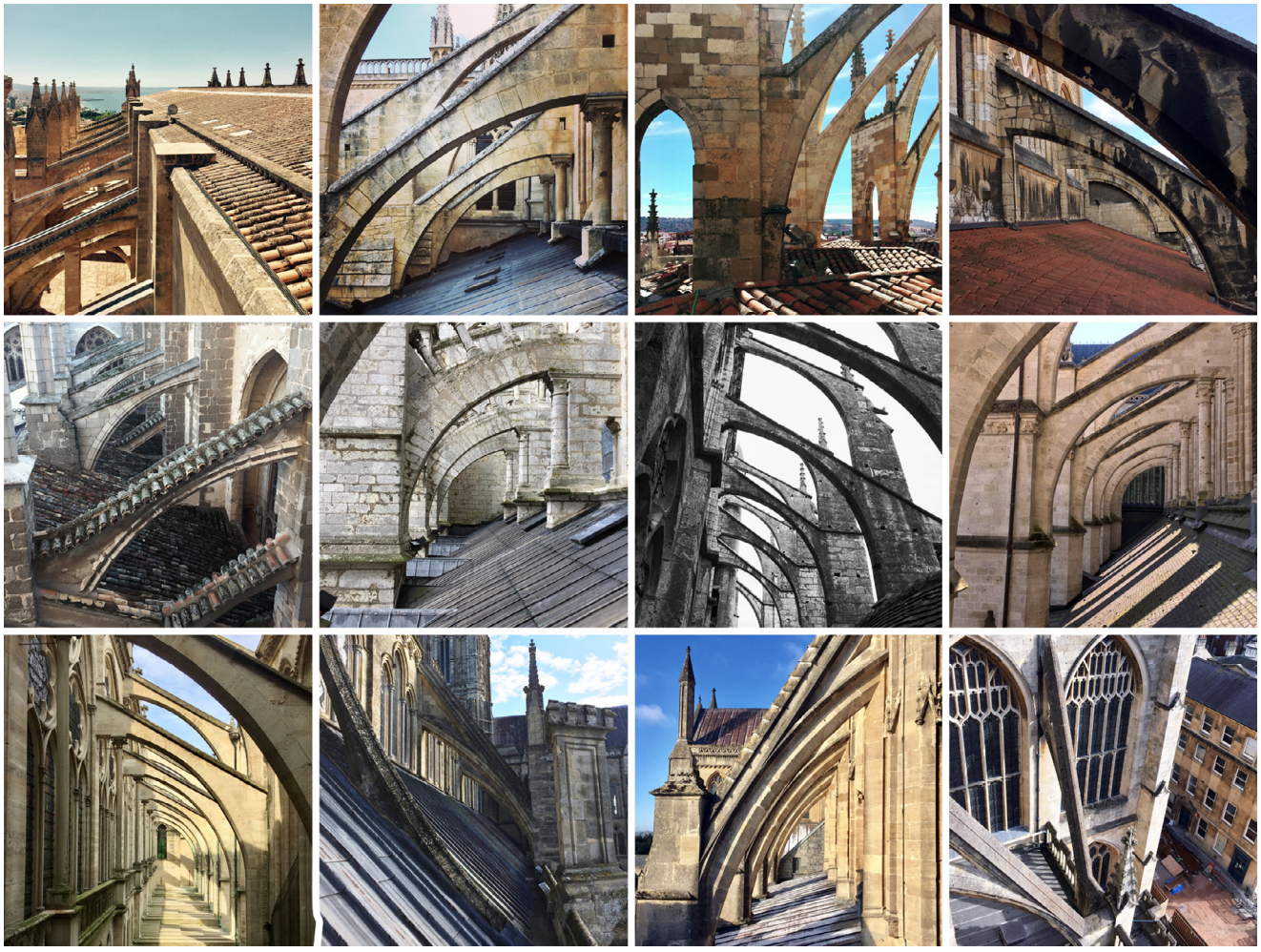

Fig. 3. Photos of the flying buttresses considered in our study. Left to right and top to bottom, they belong to the following cathedrals: Mallorca, Burgos, León, Oviedo, Toledo, Chartres, Saint Pierre in Chartres, Amiens, Saint Denis, Salisbury, Wells and Bath. [Photos taken by the authors].

Table 1
Data from the meshes for the outer surfaces of the twelve flying buttresses which have been modelled using photogrammetric techniques.

No.	Flying buttress from	Number of photos	Number of vertices	Number of faces
1	Mallorca cathedral	67	72,575	140,998
2	Burgos cathedral	76	119,537	198,295
3	León cathedral	56	49,934	96,045
4	Oviedo cathedral	44	91,038	179,999
5	Toledo cathedral	87	95,690	189,170
6	Chartres cathedral	83	78,260	155,225
7	Saint Pierre church in Chartres	40	100,560	215,890
8	Amiens cathedral	67	149,970	296,728
9	Saint Denis cathedral	61	155,567	320,135
10	Salisbury cathedral	61	85,890	168,890
11	Wells cathedral	45	89,987	176,988
12	Bath cathedral	31	49,475	97,489

Similarly, the inclination α of a flying buttress also depends on the arbitrary selection of two end points of the arch, which may result in significant differences in the value obtained.

As can be seen on the left of Fig. 2 –only as an example and exaggerating the outcome –, the arbitrary selection of two pairs of end points $\mathcal{P}_{a,b}$ and $\mathcal{P}_{c,d}$ on the edge contour of an arch results in an equally arbitrary definition and calculation of the flying buttress inclination α. The same thing happens with the rise $\mathcal{F}$ and the span $\mathcal{L}$, since they are the legs of the right triangle which determines the inclination α. On the right of Fig. 2 it can be seen that, if we draw the perpendicular bisectors of the segments resulting from the choice of any set of three points $\mathcal{P}_{e,f,j}$, $\mathcal{P}_{g,h,i}$, $\mathcal{P}_{k,m,p}$ or $\mathcal{P}_{l,n,o}$ from the edge contour of both arches, the resulting centers $\mathcal{O}_1$, $\mathcal{O}_2$, $\mathcal{O}_3$ or $\mathcal{O}_4$ are in different positions.

The subjectivity involved in the determination of the flying buttress parameters may lead to incorrect or inaccurate conclusions about the design and the construction process of this common feature of Gothic architecture.

Which is why this paper proposes a systematic method of parameter calculation which eliminates the abovementioned arbi-

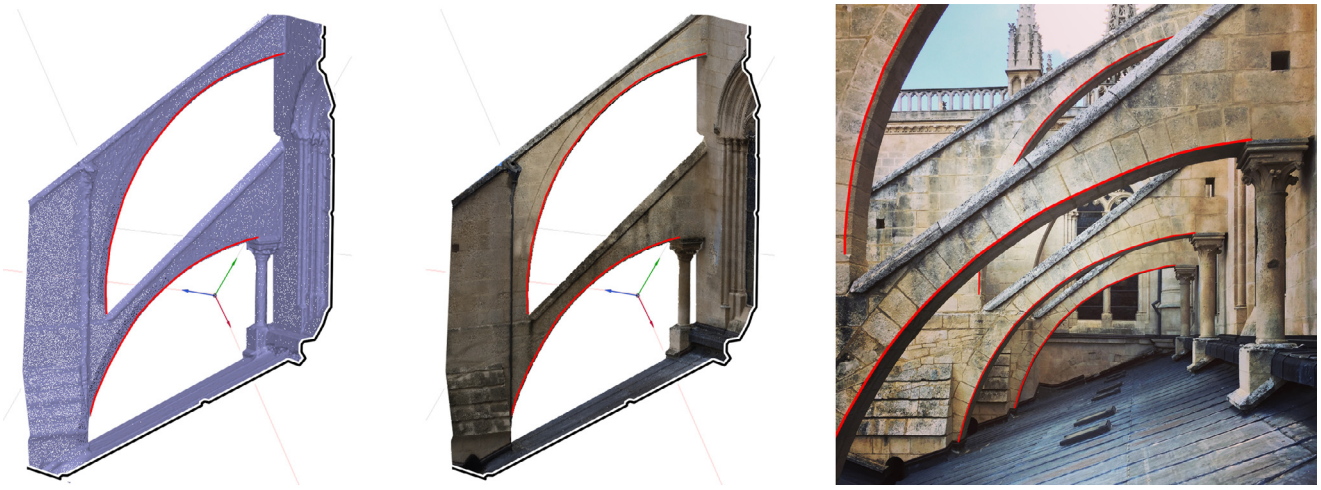

Fig. 4. Images from the photogrammetric process for the flying buttress of Burgos cathedral. On the left, the surface made up by 198,295 faces, as stated in Table 4. In the center, the texturized model. On the right, the arch edge contours $\mathcal{B}_{3-4}$ in red color. [Image generated by the authors].

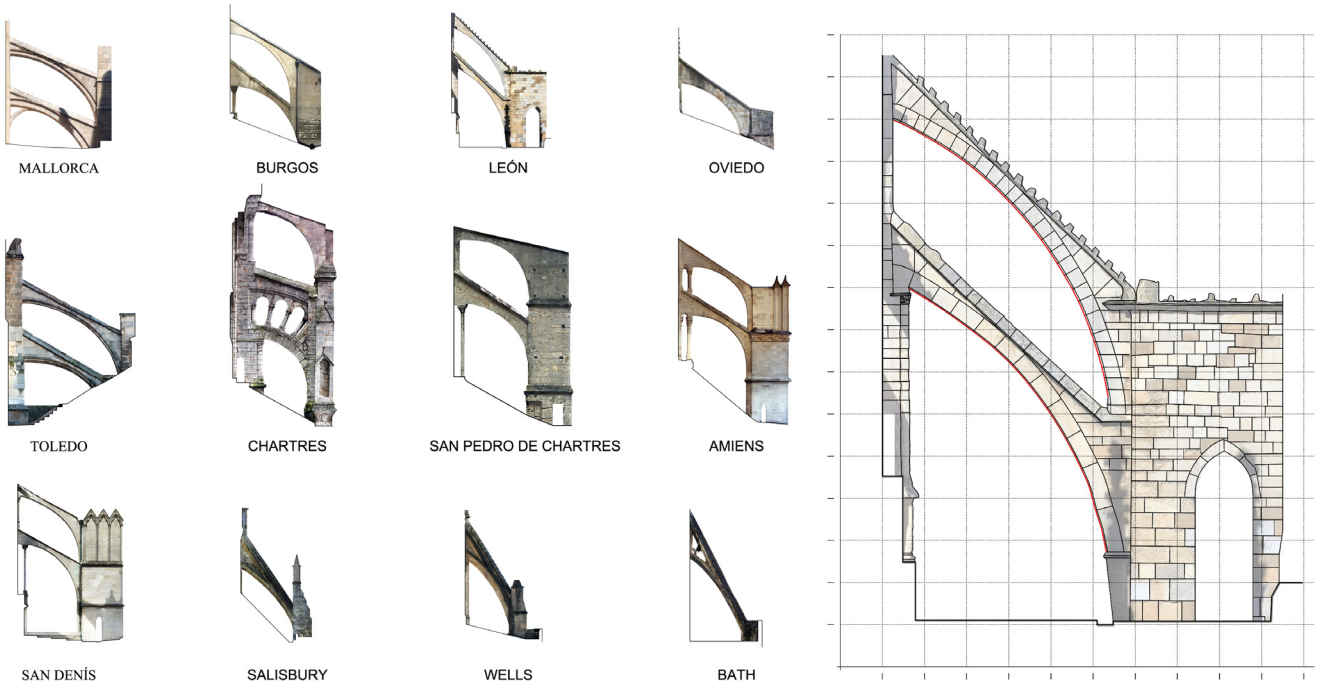

Fig. 5. On the left, the twelve texturized models. On the right, as an example, the vector drawing for the flying buttress from Leon cathedral. The arch edge contours are highlighted in red color. [Image generated by the authors].

trariness. The proposed method uses photogrammetric techniques, point cloud control, vector redrawing and geometric regression, and provides an objective, non-arbitrary procedure to determine the center $\mathcal{O}$ and the radius $\mathcal{R}$ of a flying buttress arch. This results in the following two outcomes: 1) Non-arbitrary determination of the remaining parameters α, $\mathcal{F}$, $\mathcal{L}$ and $\mathcal{E}$; 2) Non-arbitrary classification of flying buttress arches into two types, according to the criterion laid down by Viollet-le-Duc in 1854 [4, 16]; Type A): flying buttress archs with centers on the supporting wall –case O1 in Fig. 1, and Type B): flying buttress archs with centers which are displaced a certain distance δ toward the inside of the cathedral –case O2 in Fig. 1.

2. Research aim

In all buildings, particularly in architectural heritage buildings, there are certain differences between the theoretical design and the actual finished construction. Very often, the lack of historical documents detailing the design processes used by the architect to construct each element results in the building itself being the only presently available vestige which allows us to examine its construction essence or its initial theoretical design. Owing to this lack of information, together with the agents which may have altered its shape, sometimes it is not clear what theoretical principles were used by the architect to design and construct an architectural element. This paper provides an objective, non-arbitrary procedure to determine the geometric and constructive parameters which define one of the most common features of Gothic architecture: flying buttresses. As a consequence, this procedure enables all flying buttress arches to be classified according to the criterion laid down by Viollet-le-Duc in 1854, which is related to the –inner or outer– position of the arch center.

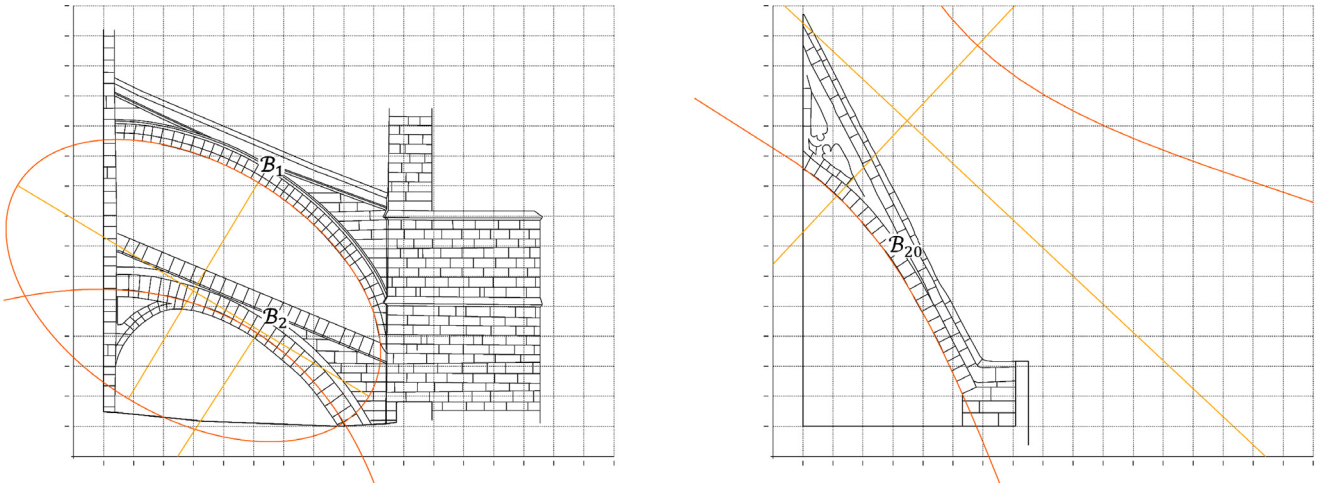

Fig. 6. On the left, the conical regression curves which fit the edge contours $\mathcal{B}_1$ and $\mathcal{B}_2$, corresponding to the arches of the flying buttress from Mallorca cathedral. On the right, the conical regression curve which fits the edge contour $\mathcal{B}_{20}$, corresponding to the arch of the flying buttress from Bath cathedral. [Image created by the authors].

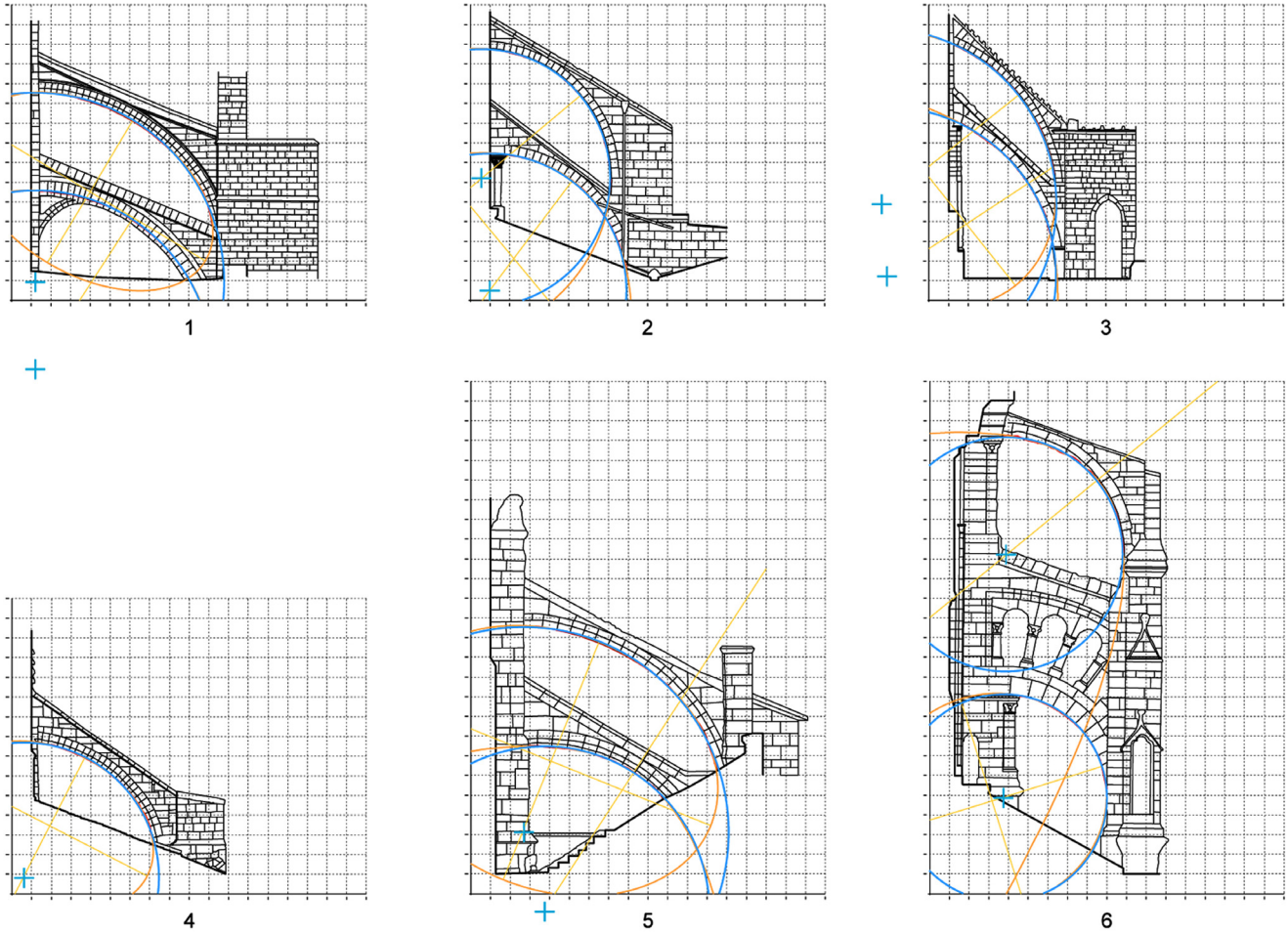

Fig. 7. Graphic results for the regression calculation of the arch edge contours $\mathcal{B}_{1-11}$. The regression circle arc is highlighted with a blue line, and the circle center $\mathcal{O}$ is marked with a cross. The conical regression curve is highlighted in orange color, and its axes are highlighted in yellow [Image created by the authors].

3. Methods

The proposed method comprises two stages: graphic determination and geometric regression. This procedure is applied to twenty arches belonging to twelve flying buttresses from twelve Gothic cathedrals –five of them in Spain, four of them in France and three of them in England (Fig. 3). The list of twelve cathedrals is as follows: Mallorca cathedral, Burgos cathedra, Leon cathedral, Oviedo cathedral, Toledo cathedral, Chartres cathedral, Saint Pierre Church in Chartres, Amiens cathedral, Saint Denis cathedral, Salisbury cathedral, Wells cathedral and Bath cathedral. As will be seen later, all the flying buttresses examined in this paper (except for those from Oviedo, Salisbury, Wells and Bath cathedrals) feature two arches –an upper arch and a lower arch.

Table 2
Parameters of the conical regression curves which fit the edge contours $\mathcal{B}_{1-20}$.

No.	Arch	a	b	ex	Type	d_γ
1	$\mathcal{B}_1$	6.825	4.200	0.788	Ellipse	99.982
1	$\mathcal{B}_2$	12.140	10.408	0.514	Ellipse	99.960
2	$\mathcal{B}_3$	7.906	7.105	0.438	Ellipse	99.976
2	$\mathcal{B}_4$	17.709	10.742	0.795	Ellipse	99.948
3	$\mathcal{B}_5$	7.483	6.151	0.569	Ellipse	99.984
3	$\mathcal{B}_6$	29.224	15.303	1.128	Hyperbola	99.905
4	$\mathcal{B}_7$	5.575	3.890	0.716	Ellipse	99.936
5	$\mathcal{B}_8$	8.769	6.499	0.671	Ellipse	99.944
5	$\mathcal{B}_9$	20.073	11.992	1.164	Hyperbola	99.877
6	$\mathcal{B}_{10}$	308.819	39.702	1.008	Ellipse	99.893
6	$\mathcal{B}_{11}$	5.854	5.411	0.381	Ellipse	99.898
7	$\mathcal{B}_{12}$	50.159	15.420	0.951	Ellipse	99.983
7	$\mathcal{B}_{13}$	5.496	4.010	0.683	Ellipse	99.958
8	$\mathcal{B}_{14}$	5.199	4.275	0.569	Ellipse	99.947
8	$\mathcal{B}_{15}$	6.173	5.569	0.431	Ellipse	99.950
9	$\mathcal{B}_{16}$	442.325	48.488	0.993	Ellipse	99.930
9	$\mathcal{B}_{17}$	5.931	5.749	0.245	Ellipse	99.960
10	$\mathcal{B}_{18}$	6.799	2.675	0.919	Ellipse	99.753
11	$\mathcal{B}_{19}$	247.103	53.595	4.718	Hyperbola	99.577
12	$\mathcal{B}_{20}$	3.421	6.219	2.074	Hyperbola	99.523

3.1. Graphic determination

This subsection deals with the first stage, which is the topographic reconstruction of the twelve flying buttreses considered in this paper. After visiting the twelve sites and taking more than seven hundred photographs –with a Canon EOS 2000D DSLR camera– in order to fully capture the outer surface of each element, a topographic reconstruction was carried out using photogrammetric techniques and the Agisoft PhotoScan Professional software product. We chose *high quality* for all steps of the photogrammetric process in order to obtain a sufficiently dense mesh to map a *high resolution* texture. Fig. 4 shows a few images from this process, and Table 1 summarizes the data for each generated model.

Based on the resulting texturized model, we have obtained a front projection of each element in TIFF format which, in turn, has allowed us to draw a linear reconstruction in CAD vector format, shown in Fig. 5.

Based on this graphic reconstruction of the twelve flying buttresses considered in our paper, we have generated a curve which outlines the edge of each arch or pair of arches, and then we have made the geometric calculations as described in the following subsection. These arch edge contours will be called $\mathcal{B}_i$, where i ranges from 1 to 20. As an example, they are shown in red color in Figs. 4 and 5.

Table 4
Statistical parameters μ, σ and CV for the sets of angle values α and the sets of thickness values $\mathcal{E}$. Row $\mathcal{B}_{1-20}$ portrays the parameters of all the arches from the flying buttresses considered in this paper, and row $\mathcal{B}_{1-17}$ only portrays the parameters of the arches from the Spanish and French flying buttresses.

	μ		σ		CV	
	α	$\mathcal{E}$	α	$\mathcal{E}$	α	$\mathcal{E}$
$\mathcal{B}_{1-20}$	43.440	3.400	8.885	0.904	0.204	0.245
$\mathcal{B}_{1-17}$	41.034	3.659	8.096	0.793	0.197	0.216

3.2. Geometric regression

While it is well established that the arches of these flying buttresses were designed using circle arcs, next are some geometric and statistical results confirming that the agents mentioned in the Introduction may have altered the original circular design shape of the arches $\mathcal{B}_{1-20}$. The procedure used to prove this involves approximating these arcs with conical curves, by means of a geometric regression. As will be described below, the best fitting curves are not circles, but ellipses or hyperbolae. Again, this is not intended to oppose the circular geometric nature of these arches, but to further stress the need to find an objective procedure to determine their inclination. As will be seen, this objective procedure is based on a circular regression.

We find the XY coordinates $(P_i = (x_i,\ y_i))$ of 10,000 points P_i which define each of the twenty arch edge contours $\mathcal{B}_{1-20}$ determined with the previously described process. This set of points is cloud $\mathcal{N}_{1-20} = \{P_i\}_{i=1}^{i=n}$, where $n = 10,000$. With the helf of a *lisp* routine called EPC, we obtain a TXT file with the coordinates of the points P_i from the clouds $\mathcal{N}_{1-20}$, and then we calculate the conical regression curve γ for each cloud.

The result of this calculation is the curve with general equation: $\gamma \equiv\ Bx^2 +\ Cy^2 + Dxy + Ex + Fy + 1 = 0$. This is the curve which best fits the cloud, minimizing the sum of the quadratic residues $\sum_{i=1}^{i=n} \varepsilon_i^2 = \sum_{i=1}^{i=n} (Bx_i^2 + Cy_i^2 + Dx_iy_i + Ex_i + Fy_i + 1)^2$. It is widely known

Table 3
Parameters of the twelve flying buttresses considered in our paper, as obtained with the geometric regression method.

No.	Arch	$\mathcal{O}$	δ	$\mathcal{R}$	α	$\mathcal{F}$	$\mathcal{L}$	$\mathcal{E}$	$\Delta\mathcal{E}$
1	$\mathcal{B}_1$	A	0.199	9.600	35.589°	6.319	8.830	4.800	−0.054
1	$\mathcal{B}_2$	A	0.199	9.058	30.764°	4.527	7.607	4.528	0.758
2	$\mathcal{B}_3$	A	0.426	6.545	49.468°	7.128	6.097	3.272	−0.133
2	$\mathcal{B}_4$	A	0.008	6.966	45.200°	6.155	6.112	3.483	0.015
3	$\mathcal{B}_5$	B	3.399	8.892	52.195°	6.557	5.087	4.446	−0.412
3	$\mathcal{B}_6$	B	3.136	8.585	52.943°	4.685	6.205	4.292	−0.223
4	$\mathcal{B}_7$	A	0.372	6.863	39.306°	4.770	5.827	3.432	−0.069
5	$\mathcal{B}_8$	A	1.415	10.404	35.425°	6.965	9.792	5.202	−0.898
5	$\mathcal{B}_9$	A	1.650	8.387	20.136°	2.526	6.890	4.193	0.305
6	$\mathcal{B}_{10}$	A	2.629	5.954	42.057°	5.464	6.057	2.977	−0.735
6	$\mathcal{B}_{11}$	A	2.473	5.257	47.789°	4.894	4.439	2.634	0.080
7	$\mathcal{B}_{12}$	A	1.991	5.682	38.595°	5.603	7.021	2.838	1.258
7	$\mathcal{B}_{13}$	A	0.694	7.128	39.909°	5.314	6.354	3.564	0.385
8	$\mathcal{B}_{14}$	A	1.808	5.441	38.138°	4.387	5.587	2.720	1.502
8	$\mathcal{B}_{15}$	A	1.759	5.309	45.270°	5.568	5.516	2.654	1.665
9	$\mathcal{B}_{16}$	A	0.578	7.030	43.772°	5.647	5.895	3.515	0.855
9	$\mathcal{B}_{17}$	A	0.067	6.075	49.239°	5.859	5.050	3.036	1.659
10	$\mathcal{B}_{18}$	B	6.277	12.605	48.854°	5.816	5.081	1.919	−0.086
11	$\mathcal{B}_{19}$	B	7.789	12.675	58.209°	6.600	4.091	1.918	0.510
12	$\mathcal{B}_{20}$	B	10.854	16.980	55.947°	7.855	5.308	2.585	0.088

that the solution to the problem of calculating γ is given by the Gauss normal equations. Specifically, we must solve the following system (1):

$$\begin{pmatrix} 1_i x_i^4 & x_i^2 y_i^2 & x_i^3 y_i & x_i^3 & x_i^2 y_i \\ x_i^2 y_i^2 & 1_i y_i^4 & x_i y_i^3 & x_i y_i^2 & y_i^3 \\ x_i^3 y_i & x_i y_i^3 & x_i^2 y_i^2 & x_i^2 y_i & x_i y_i^2 \\ x_i^3 & x_i y_i^2 & x_i^2 y_i & 1_i x_i^2 & x_i y_i \\ x_i^2 y_i & y_i^3 & x_i y_i^2 & x_i y_i & 1_i y_i^2 \end{pmatrix} \begin{pmatrix} B \\ C \\ D \\ E \\ F \end{pmatrix} = \begin{pmatrix} -1_i x_i^2 \\ -1_i y_i^2 \\ -x_i y_i \\ -1_i x_i \\ -1_i y_i \end{pmatrix} \tag{1}$$

In this equation, the range of variation for i is $i = 1 \div n$ in Einstein summation convention with repeated subscripts, being $1_i = 1$. For example: $x_i^2 y_i = \sum_{i=1}^{i=n} x_i^2 y_i$, and $1_i y_i^4 = \sum_{i=1}^{i=n} y_i^4$. The regression curves obtained for the edge contours $\mathcal{B}_{1-20}$ are displayed in Table 2. As an example, two cases are illustrated in Fig. 6. In order to ensure correct results, we have designed our own calculation software.

Table 2 shows the geometric parameters which determine the obtained conical curves γ: the curve's semi-major axis a in meters, the curve's minor transverse axis b in meters, the curve's excentricity ex, and also the type of curve, whether it is a non-circular ellipse, a circle, a parabola or a hyperbola.

Next, we will calculate to what extent each conical curve γ statistically accounts for its point cloud $\mathcal{N}$. For these calculations, we will use the well-known correlation ratio η^2, see Eq. (2):

$$\eta^2 = 1 - \frac{\sum_{i=1}^{i=n} (y_i - f(x_i))^2}{\sum_{i=1}^{i=n} \left(y_i - \bar{Y}\right)^2}, \tag{2}$$

where $\bar{Y} = \frac{1}{n} \sum_{i=1}^{i=n} y_i$, and where $(x_i,\ f(x_i))$ are the coordinates of the points forming the regression curve γ. The adjusted correlation ratio η^2_{adj} is given by Eq. (3):

$$\eta^2_{adj} = 1 - \left[\left(1 - \eta^2\right)\right] \frac{n-1}{n-5-1} \tag{3}$$

We know that $\eta^2_{adj} \in [0, 1]$, and the value $\eta^2_{adj} * 100 = d_\gamma$ is the extent to which the variables $\{y_i\}_{i=1}^{i=n}$ of cloud $\mathcal{N} = \{P_i = (x_i, y_i)\}_{i=1}^{i=n}$ are statistically explained by the least squares correlation between $\{y_i\}_{i=1}^{i=n}$ and $\{x_i\}_{i=1}^{i=n}$. In other words, this value d_γ is the percentage by which the variables $\{y_i\}_{i=1}^{i=n}$ of the points forming cloud $\mathcal{N}$ are statistically explained by the variables y of the points forming the conical curve γ. Namely, d_γ is a statistical measure of how well the regression conical curve γ fits cloud $\mathcal{N}$. Table 2 shows the d_γ values for each cloud $\mathcal{N}_{1-20}$.

The geometric and statistical results obtained by us confirm that, owing to the natural and mechanical agents mentioned in the introduction to this paper, and to the lack of accuracy during the construction process, the curves which best fit the edge contours $\mathcal{B}_{1-20}$ are *not* circle arcs. This is contrary to expectation, because these flying buttress arches were geometrically designed as circles.

The regression curves obtained are not circle arcs and, therefore, there is no objective way to choose three points in order to draw perpendicular bisectors and find the center $\mathcal{O}$ and the arc radius $\mathcal{R}$. This is why we use the regression circle, which indeed allows for an objective procedure. Thus, next we proceed to the geometric calculation of the regression circles of the clouds $\mathcal{N}_{1-20}$.

In order to calculate the regression circle θ of each cloud $\mathcal{N}_{1-20}$, the coefficients of equation $\theta \equiv\ Bx^2 +\ By^2 + Ex + Fy + 1 = 0$ must be found. The solution to this equation is the curve which best fits the cloud, minimizing the sum of the quadratic residues $\sum_{i=1}^{i=n} \varepsilon_i^2 = \sum_{i=1}^{i=n} (Bx_i^2 + By_i^2 + Ex_i + Fy_i + 1)^2$. It is widely known that the solution to the problem of calculating θ is given by the Gauss normal equations. Specifically, the following system (4) must be solved:

$$\begin{pmatrix} 1_i\left(x_i^2 + y_i^2\right)^2 & x_i\left(x_i^2 + y_i^2\right) & y_i\left(x_i^2 + y_i^2\right) \\ x_i\left(x_i^2 + y_i^2\right) & 1_i x_i^2 & x_i y_i \\ y_i\left(x_i^2 + y_i^2\right) & x_i y_i & 1_i y_i^2 \end{pmatrix} \begin{pmatrix} B \\ E \\ F \end{pmatrix} = \begin{pmatrix} -1_i\left(x_i^2 + y_i^2\right) \\ -1_i x_i \\ -1_i y_i \end{pmatrix} \tag{4}$$

Again, in order to ensure correct results we have designed our own calculation software.

4. Results

Fig. 7 and Fig. 8 below show the regression circles of the edge contours $\mathcal{B}_{1-20}$. Based on these circles, it is possible to determine the center $\mathcal{O}$ and the radius $\mathcal{R}$ of each of the twenty arches belonging to the twelve flying buttresses considered in this paper. As a consequence of the above, and by measuring parameter δ (Fig. 1), these arches can be thoroughly classified into one of the two types (A and B) laid down by Viollet-le-Duc in 1854; see Table 2.

Next, each regression circle is drawn over the corresponding flying buttress sketch and angle α is found, which is the inclination of the straight line passing through two end points which are determined on the regression circle. These end points are determined as follows: the upper end point of the regression circle arc is the point of intersection between the regression circle and the vertical straight line passing through the topmost point of the corresponding cloud N; similarly, the bottom end point is the point of intersection between the regression circle and the horizontal straight line passing through the lowermost point of the corresponding cloud N. Fig. 9 below shows a detailed view of several end points pertaining to some of the flying buttresses considered in this paper.

With regard to the calculation of the horizontal culée thickness $\mathcal{E}$, there are many literature references describing arithmetic and geometric rules to do so. Despite this, we do not know any procedure or any evidence as to which method was used by the medieval architects to determine the thickness of the culées. Therefore, for our research we propose to use the so-called one-three-point method, made popular by researchers such as Viollet, Derand or Blondel [4,17,18].

Thus, in order to determine the minimum thickness $\mathcal{E}$ of an arch's culée, a hexagon is inscribed in the circle generated by the arch. If this is done with the regression circle arcs previously determined for the considered flying buttress, the following results are observed:

1) The minimum thicknesses $\mathcal{E}_{1-17}$ calculated with the three-point method for the flying buttresses from the Spanish and French cathedrals correspond to reality quite closely or are smaller than the actual construction measurements; i.e., the real thickness $\mathcal{E}$ is larger than the minimum thickness geometrically determined by the three-point method. The average difference between both values (the real thickness and the thickness calculated with the three-point method) is 33 cm. The minimum difference is 1.5 cm for the lower arch of the flying buttress from Burgos cathedral ($\Delta\mathcal{E}_4$), and the maximum difference is 1.25 m for the upper arch of the flying buttress from Saint Pierre church in Chartres ($\Delta\mathcal{E}_{12}$). The arches having differences $\Delta\mathcal{E}_{12}$, $\Delta\mathcal{E}_{14}$, $\Delta\mathcal{E}_{15}$ and $\Delta\mathcal{E}_{17}$ differ significantly from the thickness determined by the three-point method, but in all cases the calculated culée thickness is lower than the real culée thickness $\mathcal{E}$; see Fig. 10 and Table 2.
2) The minimum calculated culée thicknesses $\mathcal{E}_{18-20}$ of the three flying buttresses from the English cathedrals turn out to be larger than the actual construction measurements.

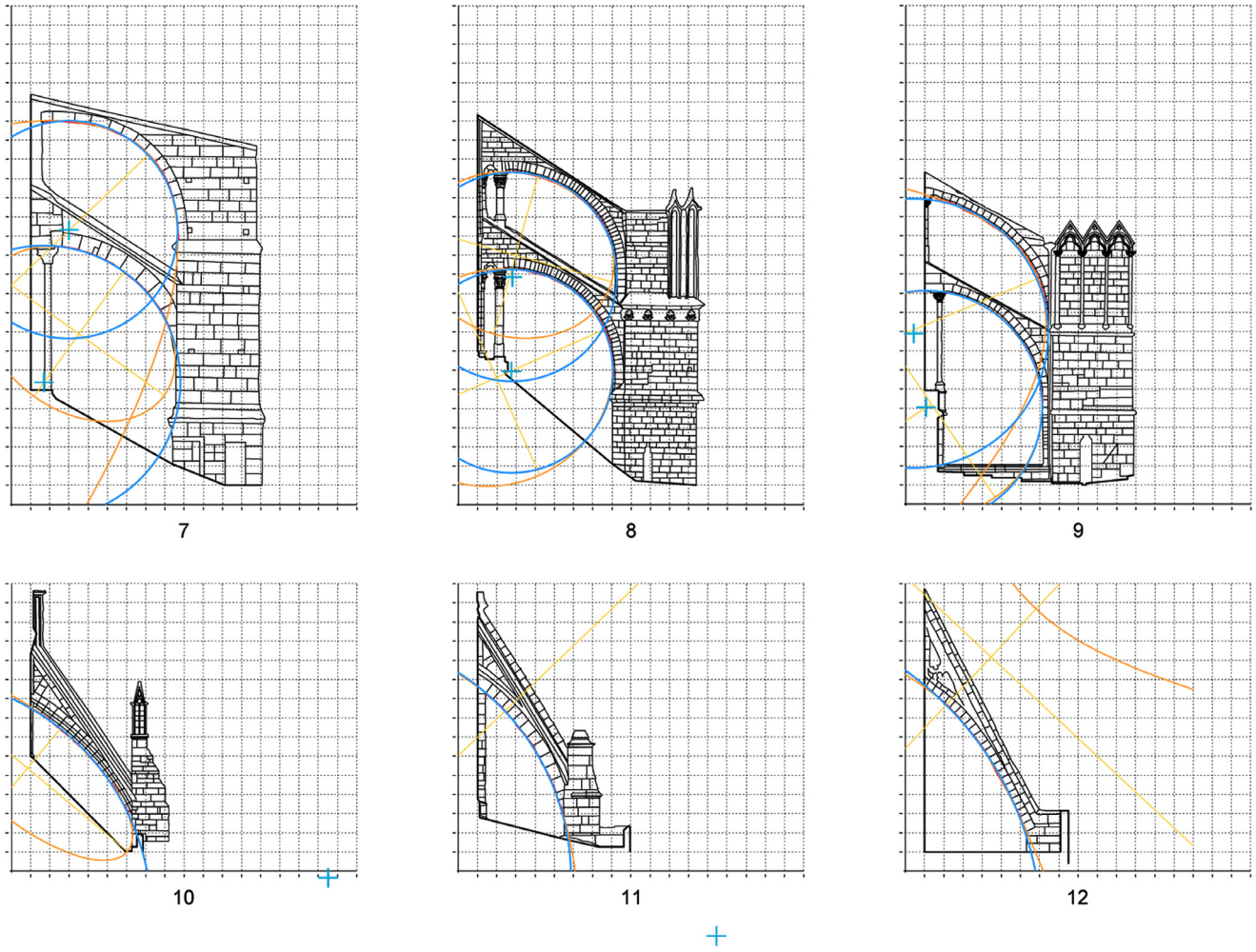

Fig. 8. Graphic results for the regression calculation of the arch edge contours $\mathcal{B}_{12-20}$. The criteria for colours are the same as in Fig. 7. [Image created by the authors].

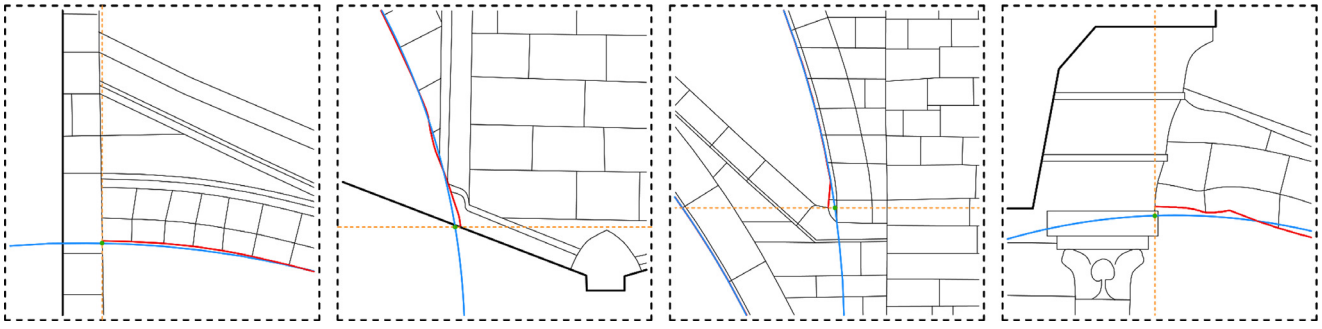

Fig. 9. Detailed view of the end points on edge contours $\mathcal{B}_1$, $\mathcal{B}_4$, $\mathcal{B}_5$ and $\mathcal{B}_{10}$. The end point of each arc on the regression circle is shown in green color. The horizontal and vertical straight lines passing through the end points (topmost end point and lowermost end point) are shown in orange color and with a dotted line.

From the point of view of statistics, given a set of parameters $C = \{p_i\}_{i=1}^{i=n}$, its Pearson's coefficient of variation CV is $CV = \frac{\sigma}{\mu}$, where $\mu = \sum_{i=1}^{i=n} \frac{p_i}{n}$ is the average of C and $\sigma = \sqrt{\sum_{i=1}^{i=n} \frac{(p_i-\mu)^2}{n}}$ is its standard deviation. In the field of statistical analysis, a set of parameters C (such as the parameters α and $\mathcal{E}$ shown in Table 2) is considered to be concentrated and have little spread if the average is representative of the whole set; and such average is usually regarded as being representative when its CV is lower than 25%.

If μ, σ and CV are calculated for the set of angle values α and the set of thickness values $\mathcal{E}$, it emerges that their CVs are lower than 25%, see Table 3. Specifically, $CV_\alpha = 20.40\%$ and $CV_\mathcal{E} = 24.50\%$. Therefore, it can be stated that the averages are a bit representative (even though not to a great extent) and the values in both sets do not show a lot of spread. Besides, if the parameters α and $\mathcal{E}$ of the three flying buttresses from the English cathedrals are excluded from the statistical analysis, it turns out that the averages are a little more representative, and the values are a bit more concentrated; the Pearson's coefficients of variation are $CV_\alpha = 19.70\%$ and $CV_\mathcal{E} = 21.60\%$.

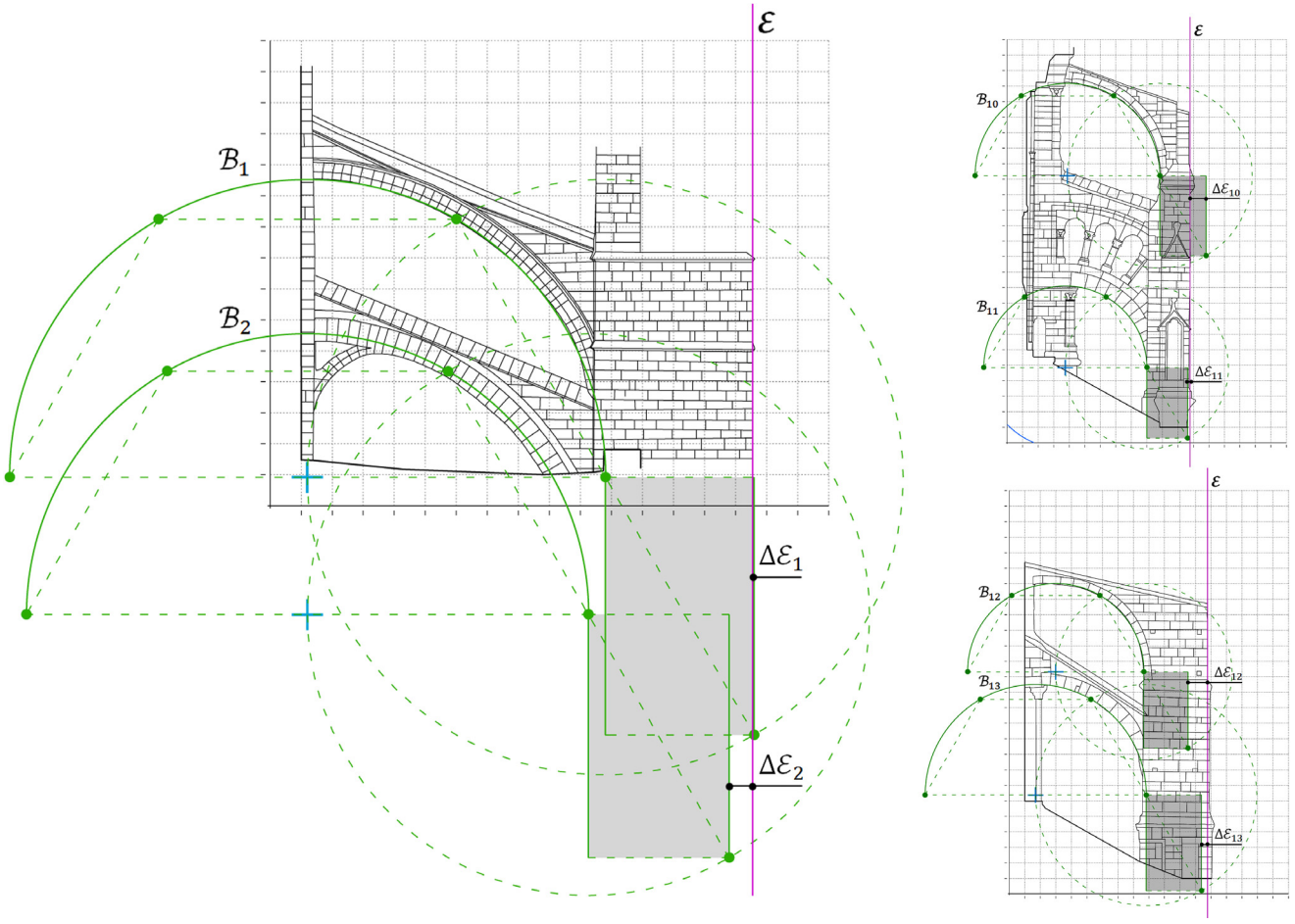

Fig. 10. In green color, we show the three-point method as applied to a few arches considered in this paper. On the left, with twice the scale of the remaining images, flying buttress from Mallorca cathedral. On the top right, flying buttress from Chartres cathedral. On the bottom right, flying buttress from Saint Pierre church in Chartres. [Image created by the authors].

5. Conclusions

This paper proposes a systematic calculation method by means of circular regression of the points pertaining to the edge contour $\mathcal{B}_n$ of a flying buttress arch. Based on this, an objective geometric method can be established to determine the arch's center $\mathcal{O}$ and the arch's radius $\mathcal{R}$. The reason for this, as we have seen, is that the traditional methods are arbitrary and may produce highly differing results.

As a direct consequence, the proposed geometric procedure enables the flying buttress arches to be classified according to the criterion laid down by Viollet-le-Duc in 1854. Throughout this paper, we have applied this method to twenty arches pertaining to twelve Gothic flying buttresses, where the three flying buttresses from English cathedrals (Salisbury, Wells and Bath) belong to type B.

The proposed method also allows to find the remaining parameters of a flying buttress (inclination α, rise $\mathcal{F}$ and span $\mathcal{L}$) in a non-arbitrary way, since these parameters are geometrically determined by the center and the radius of the flying buttress arch.

The three-point method has been used to calculate the minimum culée thickness $\mathcal{E}$ of the flying buttresses from the Spanish and French cathedrals; and it has been found that the calculated minimum thicknesses correspond to reality quite closely or are bit smaller than the actual construction measurements.

In conclusion, the lack of accuracy during the construction process, the deterioration due to the passing of time, seismic disturbances, structural distortions and other incidents of diverse nature may cause deformation of a flying buttress arch. In fact, we have shown that the curves which presently best fit the arches considered in this paper are the conical curves, and not the circle curves (even though circle curves were originally used to design the arches). For this reason, this paper defines an objective and accurate method −using a circle regression− to determine the main parameters of any flying buttress arch having one center. This method opens the door to further research on flying buttresses based on a systematic and thorough approach.

Acknowledgements

In order to carry out this research, we needed to access all the flying buttress considered in our analysis. This is why we want to thank the following people and entities: The Cathedral Chapter and Mrs Catalina Mas, Director of Mallorca Cathedral's Archive; Mr Víctor Ochotorena, churchwarden of Burgos cathedral; Mr Antonio Trobajo, Dean of Burgos Cathedral; Mr César García, historian of Oviedo Cathedral; Mr Isidoro Castañeda, Director of Toledo Primate Cathedral's archive and chapter library; Mr Gilles Fresson, Attaché de coordination of Chartres Cathedral and Saint Pierre church in Chartres; Mr Eric Charlet, Technicien des services culturels et des bâtiments de France, and Mr Antoine Paoletti, architecte des bâtiments de France et conservateur of Amiens Cathedral; Mr François-Xavier Créteaux, ingénieur des Services Culturels et du Patrimoine of Saint Denis Cathedral; Mr Gary Price, Clerk of the works of Sal-

isbury Cathedral; Mr Jez Fry, Clerk of the works of Wells Cathedral; and lastly, Mrs Sarah Fielding, Head of visitors experience in Bath Cathedral. Albert Samper and Agustí Costa-Jover are part of Serra Húnter Programme.

References

[1] S. Huerta, Geometry and equilibrium: the gothic theory of structural design, Struct. Eng. 84 (2) (2006) 23–28.
[2] R. Willis, On the Construction of the Vaults of the Middle Ages, Transactions of the Royal Institute of British Architects, London, 1842 (Vol. 1, part 2).
[3] A. Choisy, Histoire De L'architecture, 2, Gauthier-Villars, Paris, 1899.
[4] E. Viollet le Duc, Dictionnaire Raisonné de L'architecture Française du XIe Au XVIe Siècle, B. Bance, París, 1854.
[5] E. Lefèvre-Pontalis, in: Les Origines Des Arcs-Boutants, dans Congrès archéologique de France, Paris, 1919, pp. 367–396.
[6] J. Heyman, The stone skeleton, Int. J. Solids Struct. 2 (1966) 249–279.
[7] R. Mark, Experiments in Gothic Structure, The MIT Press, Cambridge, 1982.
[8] J. Fitchen, A comment on the function of the upper flying buttress in French Gothic architecture, Gazette des Beaux-Arts 45 (1955) 69–90.
[9] J. Fitchen, The Construction of Gothic Cathedrals: A study of Medieval Vault Erection, 1961 Oxford, Clarendon.
[10] P. Roca, in: Studies on the Construction of Gothic Cathedrals., Historical Constructions, P.B. Lourenço, Guimarães, 2001, pp. 71–90.
[11] S. Huerta, Las reglas estructurales del gótico tardío alemán, in: M. Arenillas, C. Segura, F. Bueno, S. Huerta (Eds.), Actas Del Quinto Congreso Nacional de Historia de La Construcción, 2007, pp. 519–532. Madrid.
[12] y I. Tarrio, Los arbotantes en el sistema de contrarresto de construcciones medievales: teorías sobre su comportamiento estructural, in: S. Huerta, P. Fuentes (Eds.), Actas Del Noveno Congreso Nacional y Primer Congreso Internacional Hispanoamericano de Historia de La Construcción, 2015, pp. 1675–1685. yMadrid.
[13] V. Quintas, Structural analysis of flying buttresses, Eur. J. Environ. Civil Eng. 21 (4) (2017) 471–507.
[14] M.K. Nikolinakou, A.J. Tallon, J.A. Ochsendorf, Structure and form of early Gothic flying buttresses, Revue Européenne de Génie Civil 9 (9–10) (2005) 1191–1217.
[15] C. Velilla, et al., Rampant arch and its optimum geometrical generation, Symmetry (Basel) 11 (5) (2019) 627.
[16] V. Llopis-Pulido, et al., Analysis of the structural behavior of the historical constructions: seismic evaluation of the cathedral of Valencia, Int. J. Architect. Heritage 13 (2019) 205–214.
[17] F. Derand, L'architecture Des Voûtes Ou L'art Des Traits Et Coupe Des Voûtes, Sebastian Cramoisy, Paris, 1643.
[18] F. Blondel, Cours D'architecture, Lambert Roulland, Paris, 1683.